HHS Public Access

Author manuscript

Pain. Author manuscript; available in PMC 2021 March 01.

Published in final edited form as:

Pain. 2020 March ; 161(3): 595–608. doi:10.1097/j.pain.0000000000001745.

Implications of the putamen in pain and motor deficits in complex regional pain syndrome

Monica Azqueta-Gavaldon[1], **Andrew M. Youssef**[2], **Claudia Storz**[1], **Jordan Lemme**[2], **Heike Schulte-Göcking**[1,3], **Lino Becerra**[2], **Shahnaz C. Azad**[3], **Anselm Reiners**[4], **Birgit Ertl-Wagner**[5], **David Borsook**[2], **Jaymin Upadhyay**[2], **Eduard Kraft**[1,3]

[1]Department of Orthopedics, Physical Medicine and Rehabilitation, University Hospital LMU Munich, Germany

[2]Department of Anesthesiology, Critical Care and Pain Medicine, Boston Children's Hospital, Harvard Medical School, Boston, MA, United States of America

[3]Interdisciplinary Pain Unit, University Hospital LMU Munich, Germany

[4]Department of Rehabilitation Medicine, City Hospital Bogenhausen, Munich, Germany

[5]Institute of Clinical Radiology, University Hospital LMU Munich, Germany

Abstract

Complex regional pain syndrome (CRPS) develops after limb injury, with persistent pain and deficits in movement frequently co-occurring. The striatum is critical for mediating multiple mechanisms that are often aberrant in CRPS, which includes sensory and pain processing, motor function and goal-directed behaviors associated with movement. Yet much remains unknown with regards to the morphological and functional properties of the striatum and its sub-regions in this disease. Thus, we investigated 20, patients (15 female, age 58 ± 9 years, right-handed) diagnosed with chronic (6+ months of pain duration) CRPS in the right hand and 20 matched, healthy controls with anatomical and resting-state, functional magnetic resonance imaging (fMRI). In addition, a comprehensive clinical and behavioral evaluation was performed, where each participant's pain, motor function and medical history were assessed. CRPS patients harbored significant abnormalities in hand coordination, dexterity and strength. These clinical pain and movement-related findings in CRPS patients were concomitant with bilateral decreases in gray matter density in the putamen as well as functional connectivity increases and decreases amongst the putamen and pre-/postcentral gyri and cerebellum, respectively. Importantly, higher levels of clinical pain and motor impairment were associated with increased putamen-pre-/postcentral gyri functional connectivity strengths. Collectively, these findings suggest that putaminal alterations, specifically the functional interactions with sensorimotor structures, may underpin clinical pain and motor impairment in chronic CRPS patients.

Corresponding Author: Monica Azqueta-Gavaldon, Marchioninistr. 15, 81377, Munich, Germany, monica.azqueta@med.uni-muenchen.de.

The authors declare that there is no conflict of interest regarding the publication of this article.

Keywords

Complex Regional Pain Syndrome; motor dysfunction; chronic pain; putamen; sensorimotor network

1 Introduction

Complex Regional Pain Syndrome (CRPS) is a pain disease that ensues following injury to an extremity [8]. The pathophysiological mechanisms that hinder a normal resolution of limb injury or unfold in CRPS phenotype are poorly understood. However, the symptoms that patients present are well-characterized, including spontaneous and movement-induced pain, sensory deficits, trophic abnormalities, and autonomic dysregulation [18]. During acute stages, soft-tissue edema, disturbed sympathetic function and movement limitation are observed. In chronic stages, motor deficits may become more defined [43], including reduced range of motion, joint stiffness, muscle weakness, tremor, dystonia, and irregular myoclonus jerks [66,67,79,91]. These movement disorders together with the observation that motor tasks that cannot be performed actively, can be executed when the affected limb is passively moved, point to a central component underlying movement-related symptomatology in CRPS [56].

Neuroimaging techniques have been used to study brain alterations in chronic pain [4,28,62]. Due to methodological and clinical divergence, the findings are difficult to summarize into consistent results. However, with respect to resting-state functional magnetic resonance imaging (rsfMRI) there is converging evidence of the disruption of the Default Mode Network (DMN) across chronic pain diseases such as low back pain [2,10], fibromyalgia [68], neuropathic diabetic pain [24], knee osteoarthritis [10] and CRPS [10,19]. Components within the DMN that exhibited changes included the medial prefrontal cortex, precuneus and lateral parietal regions. Areas outside this network such as anterior cingulate cortex, anterior insula and supramarginal gyrus also presented with alterations. Overall, changes within the DMN could be interpreted as alterations of brain function related to chronic pain, but not specific to CRPS.

Previous fMRI studies addressing pain and movement disorders in CRPS showed morphological and functional alterations localized to the primary somatosensory cortex [53,74], as well as sensorimotor network regions such as pre-and postcentral gyrus [37,56]. Past research has also focused on the cortical and thalamic contributions to pain and sensorimotor deficits in CRPS [30]. However, there has been little focus on striatal structures. This is despite the known function of the striatum in pain and motor control as well as in related processes such as reward, aversion and goal-directed behaviors [21]. Neuroanatomical evidence shows that the basal ganglia (BG), cerebellum and cerebral cortex form an integrated and topographically organized network [23]. The motor, cognitive and affective territories of each node in this network are interconnected. These observations stress the importance of subcortical contributions to neuroplasticity in chronic pain.

The role of the striatum towards facilitating persistent pain and movement-related dysfunction in CRPS was recently postulated [6]. To date, structural and functional

abnormalities in BG structures have not been studied in relation to motor dysfunction in CRPS. Therefore, in this MRI-based investigation, we aimed to elucidate the morphological and functional properties of areas within the sensorimotor network with distinct attention to the striatum in a cohort of adult chronic CRPS patients with pathology unilaterally localized to the right upper limb. We hypothesize that striatal alterations do not only affect pain processing but are also implicated in movement disorders in CRPS.

2 Material and Methods

This study was approved by the Ethics Committee of the Ludwig Maximilian University of Munich (Germany) and met the Helsinki criteria for the study of pain in humans. All subjects read and signed a written informed consent prior to study participation. Patients were recruited from the Interdisciplinary Pain Unit at the University Hospital LMU and from the Department of Rehabilitation Medicine of the City Hospital Bogenhausen in Munich (Germany). Clinical screening and MRI procedures were carried out on the same day and took place at the Department of Orthopedics, Physical Medicine and Rehabilitation and at the Institute for Clinical Radiology of the University Hospital LMU Munich, respectively. Patient recruitment and screening was carried out from April 2016 to October 2017.

2.1 Study Participants

A total of 32 potentially eligible individuals possessing CRPS were assessed for eligibility and 22 patients gave consent to participate in the study. Imaging data from two patients were discarded due to observed brain lesions. Therefore, 20 (15 females; 57.9 ± 9 years old), right-handed, chronic (6+ month of pain duration) CRPS patients unilaterally affected on the right hand or arm and right-handed, gender and age-matched healthy control subjects (N=20; 15 females; 58.5 ± 10 years old) participated in this study. The enrolled patient cohort met the Budapest clinical diagnostic criteria for CRPS [41] for chronic stage and were examined by a neurologist (E.K.). Exclusion criteria included suffering from another chronic pain condition, metabolic disorders (i.e., diabetes or hypertension), severe psychiatric comorbidities, addiction, or having any contraindications for undergoing MRI procedures.

2.2 Psychophysical Evaluation

All clinical tests were performed by an occupational therapist (C.S.) under minimal distraction in a silent room, with an ambient temperature of 25–26°C. Subjects were seated on a comfortable chair and allowed to adapt to the test environment for at least 10 minutes.

2.2.1 Motor Function Evaluation—A battery of motor behavioral tests was implemented to evaluate bilateral motor function in all chronic CRPS patients and healthy controls.

9-Hole Peg Test: Finger and hand coordination was assessed with the 9-Hole Peg Test [63], where after a trial round, participants were instructed to complete the test as fast as possible and the time needed for completion was recorded.

Forearm Range of Motion (RoM): The angular velocity (ω) in degrees/s of the forearm RoM was measured with a 3D motion tracker system based on an ultrasound probe CMS-10 (Zebris Medical GmbH, Isny Germany). During this test, patients were instructed to perform a forearm rotation at their maximum range of movement and velocity during which pronation and supination movements were recorded across a 30-second period. To account for intra-subject variability, a symmetry index (RoM_{SI}) of the angular velocity that determines side performance dominance was computed ($\omega_{right}/\omega_{left}$), where $RoM_{SI} > 1$ indicates better performance of the dominant/affected hand; $RoM_{SI} < 1$ corresponds to better performance of the left hand; and $RoM_{SI} = 1$ indicates total symmetry or equal performance between both hands.

Rigidity: The rigidity of the upper limbs was evaluated following the Unified Parkinson's Disease Rating System (UPDRS-III) measurement for rigidity [38]. Scores for each individual limb ranged from 0 – 3. The total rigidity score accounting for both limbs was calculated by the sum of the two individual scores (range 0 – 6).

Grip Strength: A vigorimeter was utilized to measure grip strength.

Right-Left Laterality Discrimination: The computer-based tool Recognize® (Neuro Orthopedic Institute, Australia) was used to assess the ability to discriminate right from left hand images and was administered on a tablet. A symmetry index was computed using the same method as described for RoM_{SI}.

Dystonia: Arm Dystonia Disability Scale (ADDS) [32] questionnaire was used to assess reported dystonia.

2.2.2 Somatosensory Evaluation—*Monofilament Test:*

Bilateral hand and finger threshold sensations were evaluated using the Semmes-Wenstein Monofilaments Examination (SWME). The monofilaments are applied to different regions of patients' hands (palmar surface of index finger and thumb, little finger and hypothenar eminence, and dorsum of the hand) perpendicularly until they bend for approximately one second. Depending on their diameter, the monofilaments can exert a pressure of 0.07, 0.4, 2, 4 or 300 g/mm^2. Having the eyes closed, patients were instructed to respond when the stimulus was felt by saying "yes". Starting with the finest monofilament, if the patients failed to feel the stimulus, the next monofilament in diameter was used for the tests. The test performance was given a clinical score of normal (Minimum force perceived = 0.07 g/mm^2), diminished light touch (Minimum force perceived = 0.4 g/mm^2), diminished protective sensation (Minimum force perceived = 2 g/mm^2), loss of protective sensation (Minimum force perceived = 4 g/mm^2), deep pressure sensation only (Minimum force perceived = 300 g/mm^2).

Two-Point Discrimination: The static two-point discrimination test was used to gauge the ability of the patients to identify two close stimulation points on a small area of the skin. The examiner randomly alternated one-point and two-point stimulation on the finger pads, while the study participants were asked to say "one" or "two" if they felt one or two points respectively. The test performance was given the clinical score of normal sensation

(Identified minimum distance = 6mm), moderately affected sensation (Identified minimum distance = 10 mm), bad sensation (Identified minimum distance = 16 mm), protective sensation (Only one point sensed).

2.2.3 Autonomic Function—The degree of autonomic dysfunction was assessed from six different perspectives. These comprised of abnormal or asymmetrical skin temperature and coloration, volume, sweat segregation, hair and nail growth. Using infrared thermometry, the skin temperature was measured three times on the bare skin, between the third and fourth metacarpal bone while avoiding the veins and hair on the dorsum of the hand, followed by three measurements on the palm of the hand. The arithmetic mean was used for further data processing and was considered to be abnormal when the temperature difference to the healthy hand was higher than 0.5°C [27]. Edema in the affected limb was assessed by measuring volume differences with the use of a hand-volumeter [64] and was classified as abnormal when the difference to the healthy limb was higher than 5% [27]. The therapist assessed sweat segregation, hair and nail growth, as well as the skin coloration through visual or/and tactile inspection.

2.2.4 Assessment of Pain, Quality of Life and Mental Health—Multiple validated self-administered questionnaires described below were completed by each participant.

Pain: Patients reported the pain intensity felt right before entering the MRI scan on a 0 – 10 visual analog scale (VAS).

Health-related quality-of-life: Health-related quality of life and disease burden was assessed with the Veterans RAND 12-item Health Survey [47]. The twelve items are summarized into two scores, a physical health (Physical Component Score, PCS) and a mental health summary measure (Mental Component Score, MCS). The PCS score ranges from 21.05 – 55.74 points, and the MCS score ranges from 12.66 – 62.88 points. For both subscales, higher scores denote better quality of life.

Depression and anxiety: Depression and anxiety status were evaluated with the German version of the Hospital Anxiety and Depression Scale (HADS-D). This 14-item self-report questionnaire comprises of two subscales (depression and anxiety) with seven items each, rated with a Likert-scale (0 – 3). The total subscale scores range from 0 – 21. The clinical cut-off score to meet the screening criteria for depression and anxiety is 8 points [17].

Kinesiophobia: Kinesiophobia or pain-related fear of movement was assessed with the 11-items Tampa Scale for Kinesiophobia (TKS-11) [92]. Items on the TSK-11 are scored from 1 (strongly disagree) to 4 (strongly agree). The total score ranges from 11 – 44 points, with higher scores indicating greater fear of pain, movement and injury. Patients with a score greater than the cut-off score of 24 are considered to have high levels of fear of movement.

2.3 Statistical Analysis (Non-imaging data)

Fulfilment of conditions of normality and homogeneity of variance of metric for psychophysical data was tested using Shapiro Wilk Test. After rejection of such fulfilment,

the Mann–Whitney U test was used to study group differences. In the case of nominal data, Fisheŕs exact test was used. The significant level was set to $\alpha = 0.05$.

2.4 Functional and Structural MRI Data Acquisition

All MRI data acquisition was performed on a 3T Siemens Magnetom Skyra MRI scanner using a 32-channel head coil (Erlangen, Germany). Anatomical MRI images were acquired using a magnetization prepared rapid gradient echo (MPRAGE) sequence. Images were obtained in a sagittal plane with a field of view of 256 mm^2 [160 1 mm-thick slices with an in-plane resolution of 1 mm (256 × 248 voxels)]. Resting-state fMRI images were acquired utilizing an echo-planar imaging (EPI) gradient echo sequence with isotropic voxels of 3.5 mm^3. Thirty-nine slices (64 × 64 in-plane resolution) were acquired per volume with TR/TE/Flip Angle = 2.5 secs/30 msecs/90° with 250 volumes.

2.5 Rationale for ROI selection

To elucidate the possible neurological pathologies underlying pain and motor deficits in CRPS, we chose to restrict our analysis to a priori selected anatomical regions of interest (ROI). We chose these regions following the rationale provided by prior publications from imaging studies in pain, CRPS and sensorimotor behavior.

Putamen is engaged in sensory-discriminative aspects of pain [21] and presents with decreased activation after treatment/symptomatic reduction in CRPS [14]. The putamen plays a crucial role in motor control and sensory integration [42].

Caudate Nucleus is part of the modulatory system of pain [33]. It presents with higher activation with nociceptive stimulation [34] and reduction after treatment [14] in CRPS. It is involved in the smooth orchestration of motor actions [82].

Nucleus Accumbens is a key component in the reward-aversion aspects of pain [60]. It is also involved in the cognitive processing of motor function related to reward and reinforcement [81].

Globus Pallidus has been demonstrated to play a role in normal motor behavior and presents with somatotopic characteristics [9]. Deep brain stimulation of this area has been reported to improve pain [55].

Thalamus is involved in the sensory discriminative and affective-motivational components of pain [1]. In pediatric CRPS, the thalamic nuclei exhibit volumetric differences in comparison with healthy controls that improve after treatment [31]. The thalamus is implicated in movement control and motor learning because it is an essential input and output node between motor areas of the cerebral cortex and motor-related subcortical structures [22].

Postcentral Gyrus has been proposed to play a significant role in the localization and discrimination of pain [26,50]. Consistent CRPS findings are alleging to reduced anatomical representation of the affected hand in this region [73] as disease progresses [58].

Insular Cortex is part of the affective circuits in pain processing [60] and, in CRPS, has been linked to higher activation during nociceptive stimulation in contrast to unaffected limb [57], as well as in comparison to healthy controls [34]. Moreover it plays a crucial role in sensorimotor integration [36].

2.6 Subcortical Gray Matter (GM) Volumetric Analysis

Using SPM12 (Wellcome Department of Imaging Neuroscience, London, UK; http://www.fil.ion.ucl.ac.uk/spm/), image pre-processing and gray matter volume probability maps were created with the Computational Anatomy Toolbox (CAT12, dbm.neuro.uni-jena.de/cat). All T1-weighted images were denoised combining Markov Random Field (MRF) method with Spatially Adaptive Non-Local Means (SALNM) filter [59,78]. The denoised images were then segmented into gray matter (GM), white matter (WM) and cerebrospinal fluid (CSF) probability maps using the Adaptive Maximum A-posterior (AMAP) technique [78], which accounts for intensity inhomogeneities, followed by the Partial Volume Estimation (PVE) [88], allowing for more precise segmentation. Linear affine transformation followed by a non-linear deformation calculated with the Diffeomorphic Anatomical Registration Through Exponentiated Lie Algebra (DARTEL) tool was used [5] to register the segmented images into the Montreal Institute Neurological (MNI-152) space. Expansion (or contraction) occurring during the spatial transformation, was corrected or “modulated” by multiplying each voxel by the Jacobian determinant derived from the spatial normalization procedure. The normalized, modulated GM images were then smoothed using an isotropic 5 mm full-width-half-maximum (FWHM) Gaussian kernel. We subsequently obtained the segmentation maps of dorsal and ventral striatum regions of interest, namely caudate nucleus, putamen, nucleus accumbens and the globus pallidus. These isolated maps were used for subsequent analysis. Both intracranial volume and age were modelled as nuisance variables in the analysis. Following an a priori primary threshold of $p < 0.001$, we applied a family-wise error rate (FWE) cluster-level extent threshold to correct for multiple comparisons. Comparisons between study group (chronic stage CRPS and matched, healthy controls) and sides (left and right) for striatal volume were conducted using group x side repeated measures ANOVA. Significant linear relationships between striatal, GM densities and psychophysical measures were determined using Pearson’s correlation analysis ($p < 0.05$).

2.7 Resting-state Functional Connectivity Analysis

2.7.1 Putaminal seed-based connectivity analysis—

Seed-based rsfMRI analyses of the putamen were done using FSL Software version 5.0 (FMRIB’s Software Library, www.fmrib.oc.ac.uk/fsl). All T-1 weighted images underwent brain extraction using Brain Extraction tool (BET) [84]. WM, GM, and CSF spatial maps were segmented using the FMRIB’s Automated Segmentation Tool (FAST) [94].

rsfMRI data underwent removal of the first four volumes; motion correction using the FMRIB’s Linear Motion Correction Tool (MCFLIRT) [45]; high pass filtered (0.01 Hz) to reduce low-frequency drift and noise effects.; spatial smoothing using a Gaussian kernel size of FWHM 5 mm, appropriate for striatal structures [25,61,86]; and grand-mean intensity normalization of the entire 4D dataset. Registration to anatomical MRI was carried out using

FMRIB's Linear Image Registration Tool (FLIRT) [46], and subsequently, registration to MNI-152 standard space was performed with FMRIB's Nonlinear Image Registration Tool (FNIRT) [3]. For further removal of motion-related artifacts, an Independent Component Analysis based strategy for Automatic Removal of Motion Artifacts (ICA-AROMA) was applied [77].

Using the normalized and smoothed images, regions where significant GM volume differences had been observed, namely left and right putamen, were used as seeds in the subsequent rsfMRI functional connectivity (rsFC) analyses. The seeds were transformed into the functional space of each subject using FLIRT. The single-subject time-series of the seeds were extracted and standardized (mean = 0; standard deviation = 1) to be used as explanatory variables (EV) in GLM analyses with the FMRIB's Improved Linear Model tool (FILM). Several confounding factors were included in the model to control for physiological noise and motion, since it is well documented that motion affects functional connectivity results [76]. These factors included WM and CSF time series, six motion parameters generated by motion correction during pre-processing (three rotation and three translation parameters) and a set of vectors identifying the time points when large motion displacements or spikes in the signal occurred. Comparisons of the connectivity maps between patients and controls were performed using Bayesian estimation for samples larger than 10 and robust outlier detection (FMRIB's Local Analysis of Mixed Effects, FLAME-1). Gender and age were included as nuisance factors in the model. Resulting group-level statistical maps were thresholded at z-value > 2.3 and a cluster significance threshold of $p = 0.05$. In statistical maps corrected for multiple comparisons, we looked for positive and negative differences.

A further general linear model was carried out to investigate possible modulatory effects of disease duration, pain levels, motor function, dystonia scores and kinesiophobia scores on putamen rsFC. The different scores of these variables were demeaned and introduced as regressors of interest in group-level analyses. All results were corrected for multiple comparisons using false discovery rate (FDR) and a cluster-size correction using a z-value > 2.3 and p-value < 0.05 statistical threshold.

2.7.2 ROI-to-ROI connectivity analysis—Given previous literature on neurological changes in chronic pain and motor deficits [2,7,11,48,72], we also explored functional connectivity properties in CRPS patients using a wider selection of seed regions involved in sensory perception and motor control. Namely: pre- and postcentral gyrus, insula, and thalamus. A ROI-to-ROI (region of interest) connectivity analysis was performed with the Functional Connectivity Toolbox (CONN-fMRI) v18.b [75] in conjunction with SPM 12. Here, preprocessed rsfMRI data underwent a component-based noise correction method [15] to reduce physiological and extraneous noise, providing interpretative information on positively and negatively correlated functional brain networks. Blood-oxygen-level-dependent (BOLD) signals from the cerebral WM and ventricles were removed using principal component analysis (PCA) of the multivariate BOLD signal within each of these masks obtained from the segmented T1-weighted MPRAGE scans. BOLD data were high pass filtered (0.01 Hz)

Seed ROIs were 10-mm-diameter spheres available from the CONN toolbox. They reproducibly represent core topological nodes within resting-state networks. Individual correlation maps were generated by extracting the mean BOLD time series from each seed ROI. Correlation coefficients with the BOLD time course of each target ROI throughout the whole brain were calculated. The resulting coefficients were converted to normally distributed scores using Fisher's transformation to obtain maps of voxel-wise functional connectivity for each seed ROI for each subject. The value of each voxel throughout the whole brain represents the relative degree of functional connectivity with each seed. These maps were subsequently used for second-level analysis of relative functional connectivity using a two-sided independent t-test to investigate differences in ROI-to-ROI connectivity between groups with a significance threshold of p=0.01.

3 Results

3.1 Pain levels and spectrum of movement-related abnormalities observed in CRPS patients.

Individual subject characteristics, disease duration, pain intensity and pain medication use are reported in Table 1. The enrolled patient population suffered from CRPS for approximately four years and possessed an average pain intensity of 5.15 ± 0.48 (mean ± standard error). Pain was distributed primarily on the distal hand and forearm. In comparison to healthy controls, CRPS patients showed significant motor impairment in the affected hand (Table 2 and Figure 1). Specifically, patients required a longer time to complete the 9-Hole Peg Test with the right hand than with the left, with 45% of the cohort at more than two standard deviations slower than the normal population. Forearm RoM results indicated that on average, patients moved their dominant forearm at a slower speed than the contralateral side. Interestingly, CRPS patients were characterized with an overall higher degree of rigidity in both the affected and unaffected hand. A little over half of the patients (55%) reported signs of dystonia. Although a number of movement-related deficits were identified in the CRPS cohort, only 30% reported high levels of kinesiophobia.

Patients did not perform worse than healthy controls in the right/left laterality discrimination task with Recognize® tool (Figure 1). However, somatosensory evaluation during monofilament stimulation revealed a significantly decreased sensitivity in the right hand of CRPS patients when compared to healthy controls (Table 2). Hyperhidrosis (95%), edema (60%) and vasomotor (70%) changes were present in most of the patients. CRPS diagnosis was also associated with symptoms resulting from trophic changes such as nail growth atrophy and less than half of the individuals showed skin temperature differences or abnormal hair growth patterns. CRPS patients reported significantly lower quality-of-life scores than healthy controls, in both physical and mental status. Results of the depression and anxiety scales indicated that the percentage of CRPS patients meeting the criteria for depression and anxiety was higher than in healthy controls (depression, CRPS: 45%, controls: 0%; anxiety, CRPS: 35%, healthy controls: 10%). The enrolled patients reported low levels of fear of movement, and only 30% reported high levels of kinesiophobia.

3.2 Decreases in putaminal GM volume observed in CRPS.

In comparison to healthy controls, a significant, bilateral decrease in putaminal GM volume in chronic CRPS patients was measured (Figure 2, Table 3). A negative association (Pearsońs correlation) was quantified between GM densities of the left putamen (contralateral to the affected hand in CRPS patients) and forearm mobility measured with the RoM test ($r = -0.46$, $p = 0.043$). Additionally, greater left compared to right hemisphere volumes were detected for caudate nucleus and globus pallidus across the two study cohorts.

3.3 Putamen-based functional connectivity strength associated with motor impairment in CRPS.

Following the observed decreased GM density of the putamen in CRPS patients, single-subject time series were extracted from this striatal sub-region (separately for left and right hemisphere) for subsequent seed-region, functional connectivity analyses. Head motion for all study participants during rsfMRI was first analyzed. Subjects (N=40) did not display an absolute head motion greater than 2 mm, and therefore, no imaging dataset was omitted in the analysis. Moreover, a t-test comparing mean displacement between groups showed no group-level differences (mean ± standard error, CRPS: 0.36 ± 0.037 mm; controls: 0.29 ± 0.049 mm, $p = 0.25$). The CRPS cohort compared to matched controls demonstrated significantly greater functional connectivity strength amongst the right (ipsilateral to the affected limb) putamen and sensorimotor (pre-/postcentral gyri) and superior parietal cortices, while decreased connectivity was quantified within crus I region of the cerebellum; a cerebellar node implicated in pain processing (Figure 3, Table 4) [65].

Interaction analyses involving parameters informing on motor impairment, revealed a significant profound effect between the putamen and areas involved in information processing and motor fine-tuning. Specifically, patients with poorer finger and hand coordination performance, as determined by the 9-Hole Peg Test, showed decreased functional connectivity between the left putamen and both the cerebellum (crus I and II) and precuneus, the latter of which connects to supplementary motor, premotor cortex and somatosensory cortices (Figure 4, Table 4). Patients with diminished forearm RoM presented with decreased connectivity between the left putamen and primary sensorimotor areas (Table 4, Supplemental Figure 1A), while connectivity strengths of the left putamen to the supramarginal gyrus were positively correlated with a higher degree of dystonia (Table 4, Supplemental Figure 1B). Patient specific, pain intensity ratings acquired just prior to the scan session were used in secondary regression analysis. Here, higher clinical pain levels showed greater putamen (left hemisphere)-based connectivity along the length of the left pre-/postcentral gyrus (Supplemental Figure 1C). This cortical region topologically corresponded to the hand and arm representation within the primary sensorimotor cortex. However, when further correcting these results for multiple comparisons with false discovery rate (FDR), only the correlations with the 9-Hole Peg Test were significant.

3.4 Decreased functional connectivity in motor networks

Results of the exploratory ROI-to-ROI connectivity analysis are depicted in supplementary material (Supplemental Table 1, Supplemental Figure 2). The CRPS cohort compared to matched, healthy controls demonstrated decreased functional connectivity strength amongst

the left postcentral gyrus and the precuneus and the ipsilateral hippocampus. On the other hand, the left postcentral gyrus showed increased connectivity with the contralateral frontal operculum. Decreased functional connectivity was quantified between the right and left insular cortex and vermis IX and crus II of the cerebellum, respectively. Left thalamus also exhibited decreased functional connectivity with the cerebellar vermis VII and VIII.

4 Discussion

4.1 Sensorimotor Changes in CRPS

This investigation characterized the clinical profile along with morphological and functional properties of sensorimotor network nodes with particular emphasis on the putamen in a cohort of chronic CRPS patients. In addition to a moderate level of pain, CRPS patients, relative to healthy controls, displayed multiple motor, somatosensory and autonomic abnormalities localized to the affected limb. The most prominent motor impairments observed, namely weakness, reduced distal arm mobility and limited coordination are in agreement to what has been previously reported [43]. Dystonia, which was reported by over half of the CRPS cohort, has been related to neuropathological defects in the basal ganglia [69], and is a common symptom for CRPS [66]. The symptomatic presentation of the enrolled patient population is comparable to that which is typically observed [16]. In contrast to previous studies with rsfMRI methodology on CRPS, our patients were carefully selected for unilateral distribution of ongoing pain and existing motor impairment of the dominant hand.

4.2 Putaminal and Sensorimotor Cortical Changes in CRPS

Neuroimaging data revealed bilateral decreases in putaminal volume in CRPS patients, which is in accord with recent meta-analysis findings of different chronic pain cohorts [83], and with findings specific to CRPS [11]. Decreased volume in the putamen might have a negative impact in motor function, as it is the case in Parkinson’s Disease [70]. Volumetric decreased in nucleus accumbens in CRPS previously reported [35], was not replicated in our structural MRI results. Nevertheless, a parallel trend in ventral striatum across the two investigations of nearly equal sample sizes (N~20) was observed.

Putamen-based, functional connectivity differences between the two cohorts were unilaterally observed in the right cerebral hemisphere (ipsilateral to the affected hand), implicating the ipsilateral somatosensory and association cortices, as well as cerebellar cortices. Though ipsilateral hemispheric changes might seem counterintuitive, such reorganization of components of the cortical pain connectome has been observed in multiple chronic pain studies [39,71]. These observations might be the result of extensive use of the non-dominant but healthy limb. However, the specific relevance of this ipsilateral functional connectivity change of the putamen to pre-/postcentral gyrus needs to be further elucidated. Previous studies using task-dependent fMRI for investigating motor behavior in CRPS have not frequently reported changed activity in the putamen or other parts of the striatum. However, a recent study noted reduced neural responses within the putamen and nucleus accumbens in CRPS patients performing a mental rotation task, which incorporates motor and goal-directed processes to CRPS neuropathology [51]. Given the specific motor

disorders displayed in CRPS patients including hypokinesia and dystonia, it is conceivable that a more in-depth comparison between a motor and a sensory task may clarify whether altered functional connectivity of the putamen is explained by the motor-related abnormalities or pain-related processing.

From regression analyses of neuroimaging data, the relationships between properties of the putamen (contralateral to the affected limb) with clinical pain and measures of motor function were realized and showed similar involvement of structures, namely pre-/postcentral gyrus. Changes involving the cortical sensorimotor network are in line with earlier works and seem to be related to motor impairment or a maintained fear of pain and movement avoidance in children [13]. It is also worth discussing the conflicting results of decreased putaminal volume in conjunction with altered functional connectivity with sensorimotor regions. This phenomenon is also observed in motor disorders related to neurodegeneration of the nigrostriatal pathways [44]. This result could represent a (relative) overactivity of residual neurons in the putamen yielding either increases or decreases in functional connectivity with cortical regions.

The most robust finding when titrated down was finger coordination associated with decreased connectivity between the contralateral putamen and precuneus as well as parietal association areas in CRPS. The precuneus is involved in integration of information and perception of the environment. It is an important hub of the DMN with a role in self-consciousness. Alterations in the precuneus and greater DMN have been shown to contribute significantly to pain miss-processing in migraine [20], motor dysfunction in Parkinson’s disease [87], as well as in CRPS [10].

Interestingly, in healthy volunteers undergoing sustained pressure pain, connectivity between the putamen and pre-/postcentral gyrus was negatively correlated with pain intensity [49], which is in contrast to our observations. This disparity potentially suggests differences in processing of pain in healthy volunteers and CRPS patients, but perhaps it may also a distinction between experimental versus clinical pain. Moreover, hypersensitivity to cold and brush stimuli applied to the affected CRPS limb have been reported to implicate the caudate as well as the putamen [52,54]. Yet, recent data solely involving healthy volunteers suggests that this may not be specific to CRPS, but rather a feature that extends to the general population, as well as to transiently evoked pain or hyperalgesic states [40].

Our findings localized to the putamen likely suggest an involvement of the reward-aversion system in CRPS, which is expected considering that persistent pain is a robust, aversive stimuli [93]. Moreover, the putamen is an integral component of both the dopamine and opioid receptor systems, which play a role in reward processes such as analgesia [21,90]. Thus, functional and structural modulation of the putamen may not only underpin enhanced aversion-related processes, but the same alterations may pose barriers to experiencing reward or analgesia.

A more widespread functional connectivity analysis (ROI-to-ROI) involving critical areas for motor control and pain showed a generalized decreased connectivity to the sensorimotor cerebellum (Crus I, II and vermis VIII) and to the cognitive network of the cerebellum

(vermis IX) [85]. The cerebellum plays an essential role in pain modulation and cognitive control [29]. Changes in connectivity involving the cerebellum with the insula and putamen may further point to deficits in integrating sensorimotor information with affective processing in CRPS. Alterations within motor regions in relation to changes within the cerebellum have also been reported in chronic pain conditions and may add to the known function of the cerebellum and how it coordinates with altered sensory-motor and emotional processing in the presence of chronic pain [62]. Moreover, decreased connectivity between postcentral gyrus and precuneus was revealed. These two regions are densely interconnected [89], and the observed connectivity changes may be related to alterations within the DMN or salience networks in response to chronic pain in CRPS patients. This is in agreement with findings in other chronic pain conditions. The functional relevance of the connectivity between postcentral gyrus and hippocampus has been related to perceptual cues [80]. Therefore, the observed decreased connectivity between these two regions may suggest impaired perceptual processing of sensory information in CRPS patients.

Altered activity within the primary somatosensory cortex and posterior insular cortex has been observed across several chronic pain diseases in presence of noxious stimuli, which suggests aberrant intensity processing of pain in chronic pain states [62]. Thus, our results involving these cortical areas might be related to chronic pain in general and not specific to CRPS. Alterations within the basal ganglia, particularly in the putamen, have been suggested to pertain to altered motor and general connectivity of the brain in chronic pain [12]. In our study, we were able to show that changes in the putamen correlated with diminished motor control, corroborating this suggestion.

4.3 Caveats

There are several caveats to consider: *Study Design*: Given the nature of this cross-sectional study, it remains difficult to confirm if the current putamen based functional changes are reflective of pathophysiological changes or adaptive processes in CRPS. To disentangle these two intertwined phenomena, future studies may involve a task-based paradigm as well as longitudinal study designs. Such approaches may help to differentiate CNS findings that are pathologic versus those that are perhaps compensatory mechanisms by which ‘healthy’ CNS pathways are recruited to maintain some level of normal function. *Medication Effects:* Efforts in future investigations in acute or chronic CRPS patients should better control the amount or type of medication consumed. A washout period prior to a clinical imaging examination may be valuable to implement. *Putaminal Changes in other pain conditions*: A limitation of the present study is that the findings might not be specific to CRPS [21]. Therefore, comparison with other chronic pain population, preferably such with chronic hand pain of other origin such as carpal tunnel syndrome might be more appropriate than healthy controls.

4.4 Conclusions

Undisputable, the central nervous system (CNS) contributes to pain and motor impairments in CRPS. To date, past investigations have predominately alluded to and focused upon a significant cortical network involvement in the pain processing aspects of CRPS [34,48]. Our most robust findings implicate changes in the putamen, suggesting that the striatum

might be also an essential component in motor network differences previously shown [19,56] and is a crucial component in the chronic CRPS phenotype. This is especially evident when viewing both the structural and functional neuroimaging results in the context of well-known clinical and motor function profiles of this chronic pain condition.

Supplementary Material

Refer to Web version on PubMed Central for supplementary material.

5 Acknowledgements

We would like to thank all the CRPS patients and healthy volunteers that participated in this study.

6 References

[1]. Ab Aziz CB, Ahmad AH. The role of the thalamus in modulating pain. Malaysian J Med Sci 2006;13:11–18.

[2]. Alshelh Z, Marciszewski KK, Akhter R, Di Pietro F, Mills EP, Vickers ER, Peck CC, Murray GM, Henderson LA. Disruption of default mode network dynamics in acute and chronic pain states. NeuroImage Clin 2018;17:222–231. doi:10.1016/j.nicl.2017.10.019. [PubMed: 29159039]

[3]. Andersson JLR, Jenkinson M, Smith S, Andersson J. Non-linear registration aka Spatial normalisation FMRIB Technial Report TR07JA2. 2007 p. Available: http://www.fmrib.ox.ac.uk/datasets/techrep/tr07ja2/tr07ja2.pdf Accessed 14 Nov 2017.

[4]. Apkarian AV, Bushnell MC, Treede R-D, Zubieta J-K. Human brain mechanisms of pain perception and regulation in health and disease. Eur J Pain 2005;9:463–84. doi:10.1016/j.ejpain.2004.11.001. [PubMed: 15979027]

[5]. Ashburner J. A fast diffeomorphic image registration algorithm. Neuroimage 2007;38:95–113. doi:10.1016/J.NEUROIMAGE.2007.07.007. [PubMed: 17761438]

[6]. Azqueta-Gavaldon M, Schulte-Göcking H, Storz C, Azad S, Reiners A, Borsook D, Becerra L, Kraft E. Basal ganglia dysfunction in complex regional pain syndrome - A valid hypothesis? Eur J Pain 2017;21:415–424. doi:10.1002/ejp.975. [PubMed: 27805769]

[7]. Bailey J, Nelson S, Lewis J, McCabe CS. Imaging and clinical evidence of sensorimotor problems in CRPS: utilizing novel treatment approaches. J Neuroimmune Pharmacol 2013;8:564–75. doi:10.1007/s11481-012-9405-9. [PubMed: 23054370]

[8]. Bailey J, Nelson S, Lewis J, McCabe CS. Imaging and Clinical Evidence of Sensorimotor Problems in CRPS: Utilizing Novel Treatment Approaches. J Neuroimmune Pharmacol 2013;8:564–575. doi:10.1007/s11481-012-9405-9. [PubMed: 23054370]

[9]. Baker KB, Lee JYK, Mavinkurve G, Russo GS, Walter B, DeLong MR, Bakay RAE, Vitek JL. Somatotopic organization in the internal segment of the globus pallidus in Parkinson's disease. Exp Neurol 2010;222:219–225. [PubMed: 20059997]

[10]. Baliki MN, Mansour AR, Baria AT, Apkarian AV. Functional Reorganization of the Default Mode Network across Chronic Pain Conditions. PLoS One 2014;9:e106133. doi:10.1371/journal.pone.0106133.

[11]. Barad MJ, Ueno T, Younger J, Chatterjee N, Mackey S. Complex Regional Pain Syndrome Is Associated With Structural Abnormalities in Pain-Related Regions of the Human Brain. J Pain 2014;15:197–203. doi:10.1016/j.jpain.2013.10.011. [PubMed: 24212070]

[12]. Becerra L, Morris S, Bazes S, Gostic R, Sherman S, Gostic J, Pendse G, Moulton E, Scrivani S, Keith D, Chizh B, Borsook D. Trigeminal neuropathic pain alters responses in CNS circuits to mechanical (brush) and thermal (cold and heat) stimuli. J Neurosci 2006;26:10646–10657. [PubMed: 17050704]

[13]. Becerra L, Sava S, Simons LE, Drosos AM, Sethna N, Berde C, Lebel AA, Borsook D. Intrinsic brain networks normalize with treatment in pediatric complex regional pain syndrome. NeuroImage Clin 2014;6:347–69. doi:10.1016/j.nicl.2014.07.012. [PubMed: 25379449]

[14]. Becerra L, Schwartzman RJ, Kiefer RT, Rohr P, Moulton EA, Wallin D, Pendse G, Morris S, Borsook D. CNS Measures of Pain Responses Pre- and Post-Anesthetic Ketamine in a Patient with Complex Regional Pain Syndrome. 1526. doi:10.1111/j.1526-4637.2009.00559.x.

[15]. Behzadi Y, Restom K, Liau J, Liu TT. A component based noise correction method (CompCor) for BOLD and perfusion based fMRI. Neuroimage 2007;37:90–101. doi:10.1016/j.neuroimage.2007.04.042. [PubMed: 17560126]

[16]. Birklein F, Dimova V. Complex regional pain syndrome–up-to-date. PAIN Reports 2017:1. doi:10.1097/PR9.0000000000000624.

[17]. Bjelland I, Dahl AA, Haug TT, Neckelmann D. The validity of the Hospital Anxiety and Depression Scale. An updated literature review. J Psychosom Res 2002;52:69–77. Available: http://www.ncbi.nlm.nih.gov/pubmed/11832252 Accessed 28 Sep 2018. [PubMed: 11832252]

[18]. Boerl RDH, Marinusl J, Hiltenl JJ, Huygenl FJ, Eijsl F, Kleefl M, Bauerl MCR, Gestell M, Zuurmondl WWA, Perezl RSGM. Distribution of signs and symptoms of Complex Regional Pain Syndrome type I in patients meeting the diagnostic criteria of the International Association for the Study of Pain. Eur J Pain 2011;15:830e1–830.e8. doi:10.1016/j.ejpain.2011.01.012. [PubMed: 21334934]

[19]. Bolwerk A, Seifert F, Maihöfner C. Altered Resting-State Functional Connectivity in Complex Regional Pain Syndrome. J Pain 2013;14:1107–1115.e8. doi:10.1016/j.jpain.2013.04.007. [PubMed: 23791136]

[20]. Borsook D, Maleki N, Burstein R. Migraine. Neurobiol Brain Disord 2015:693–708. doi:10.1016/B978-0-12-398270-4.00042-2.

[21]. Borsook D, Upadhyay J, Chudler EH, Becerra L. A Key Role of the Basal Ganglia in Pain and Analgesia - Insights Gained through Human Functional Imaging. Mol Pain 2010;6:1744–8069-6–27. doi:10.1186/1744-8069-6-27.

[22]. Bosch-Bouju C, Hyland BI, Parr-Brownlie LC. Motor thalamus integration of cortical, cerebellar and basal ganglia information: Implications for normal and parkinsonian conditions. Front Comput Neurosci 2013.

[23]. Bostan AC, Strick PL. The basal ganglia and the cerebellum: nodes in an integrated network. Nat Rev Neurosci 2018;19:338–350. doi:10.1038/s41583-018-0002-7. [PubMed: 29643480]

[24]. Cauda F, Sacco K, Duca S, Cocito D, D'Agata F, Geminiani GC, Canavero S. Altered Resting State in Diabetic Neuropathic Pain. PLoS One 2009;4:e4542. doi:10.1371/journal.pone.0004542.

[25]. Choi EY, Yeo BTT, Buckner RL. The organization of the human striatum estimated by intrinsic functional connectivity. J Neurophysiol 2012;108:2242–2263. doi:10.1152/jn.00270.2012. [PubMed: 22832566]

[26]. Craig ADB. Pain mechanisms: labeled lines versus convergence in central processing. Annu Rev Neurosci 2003;26:1–30. doi:10.1146/annurev.neuro.26.041002.131022. [PubMed: 12651967]

[27]. Davidoff G, Morey K, Amann M, Stamps J. Pain measurement in reflex sympathetic dystrophy syndrome 21. Pain 1988;32:27–34. Available: https://pdfs.semanticscholar.org/bd5b/7db87eeeb3e28b4228e76e0f4da9a4c5a253.pdf Accessed 14 Nov 2017. [PubMed: 3340421]

[28]. Davis KD. Introduction to a Special Issue on Innovations and Controversies in Brain Imaging of Pain. PAIN Reports 2019;4:e771.

[29]. Diano M, D'agata F, Cauda F, Costa T, Geda E, Sacco K, Duca S, Torta DM, Geminiani GC. Cerebellar Clustering and Functional Connectivity During Pain Processing. n.d. doi:10.1007/s12311-015-0706-4.

[30]. Drummond PD. Sensory Disturbances in Complex Regional Pain Syndrome: Clinical Observations, Autonomic Interactions, and Possible Mechanisms. Pain Med 2010;11:1257–1266. doi:10.1111/j.1526-4637.2010.00912.x. [PubMed: 20704674]

[31]. Erpelding N, Simons L, Lebel A, Serrano P, Pielech M, Prabhu S, Becerra L, Borsook D. Rapid treatment-induced brain changes in pediatric CRPS. Brain Struct Funct 2016;221:1095–111. doi:10.1007/s00429-014-0957-8. [PubMed: 25515312]

[32]. Fahn S. Assessment of the primary dystonias In: Munsat TL, editor. Quantification of Neurologic Deficit. Oxford: Butterworths, 1989 pp. 241–270.

[33]. Freund W, Klug R, Weber F, Stuber G, Schmitz B, Wunderlich AP. Perception and suppression of thermally induced pain: a fMRI study. Somatosens Mot Res 2009;26:1–10. doi:10.1080/08990220902738243. [PubMed: 19283551]

[34]. Freund W, Wunderlich AP, Stuber G, Mayer F, Steffen P, Mentzel M, Weber F, Schmitz B. Different Activation of Opercular and Posterior Cingulate Cortex (PCC) in Patients With Complex Regional Pain Syndrome (CRPS I) Compared With Healthy Controls During Perception of Electrically Induced Pain: A Functional MRI Study. Clin J Pain 2010;26:339–347. doi:10.1097/AJP.0b013e3181cb4055. [PubMed: 20393270]

[35]. Geha PY, Baliki MN, Harden RN, Bauer WR, Parrish TB, Apkarian AV. The brain in chronic CRPS pain: abnormal gray-white matter interactions in emotional and autonomic regions. Neuron 2008;60:570–81. doi:10.1016/j.neuron.2008.08.022. [PubMed: 19038215]

[36]. Ghaziri J, Tucholka A, Girard G, Boucher O, Houde JC, Descoteaux M, Obaid S, Gilbert G, Rouleau I, Nguyen DK. Subcortical structural connectivity of insular subregions. Sci Rep 2018;8.

[37]. Gieteling EW, van Rijn MA, de Jong BM, Hoogduin JM, Renken R, van Hilten JJ, Leenders KL. Cerebral activation during motor imagery in complex regional pain syndrome type 1 with dystonia. Pain 2008;134:302–309. doi:10.1016/j.pain.2007.04.029. [PubMed: 17561345]

[38]. Goetz CG, Tilley BC, Shaftman SR, Stebbins GT, Fahn S, Martinez-Martin P, Poewe W, Sampaio C, Stern MB, Dodel R, Dubois B, Holloway R, Jankovic J, Kulisevsky J, Lang AE, Lees A, Leurgans S, LeWitt PA, Nyenhuis D, Olanow CW, Rascol O, Schrag A, Teresi JA, van Hilten JJ, LaPelle N. Movement Disorder Society-sponsored revision of the Unified Parkinson's Disease Rating Scale (MDS-UPDRS): Scale presentation and clinimetric testing results. Mov Disord 2008;23:2129–2170. doi:10.1002/mds.22340. [PubMed: 19025984]

[39]. Gustin SM, Peck CC, Cheney LB, Macey PM, Murray GM, Henderson LA. Pain and Plasticity: Is Chronic Pain Always Associated with Somatosensory Cortex Activity and Reorganization? J Neurosci 2012;32:14874–14884. doi:10.1523/JNEUROSCI.1733-12.2012. [PubMed: 23100410]

[40]. Hansen MS, Asghar MS, Wetterslev J, Pipper CB, Mårtensson J, Becerra L, Christensen A, Nybing JD, Havsteen I, Boesen M, Dahl JB. The association between areas of secondary hyperalgesia and volumes of the caudate nuclei and other pain relevant brain structures-A 3-tesla MRI study of healthy men. PLoS One 2018;13:e0201642. doi:10.1371/journal.pone.0201642.

[41]. Harden RN, Bruehl S, Perez RSGM, Birklein F, Marinus J, Maihofner C, Lubenow T, Buvanendran A, Mackey S, Graciosa J, Mogilevski M, Ramsden C, Chont M, Vatine J-J. Validation of proposed diagnostic criteria (the "Budapest Criteria") for Complex Regional Pain Syndrome. Pain 2010;150:268–74. doi:10.1016/j.pain.2010.04.030. [PubMed: 20493633]

[42]. Hening W, Harrington DL, Poizner H. Basal Ganglia: Motor Functions of Encyclopedia of Neuroscience. Berlin, Heidelberg: Springer Berlin Heidelberg, n.d. pp. 346–350. doi:10.1007/978-3-540-29678-2_561.

[43]. Van Hilten JJ. Movement Disorders in Complex Regional Pain Syndrome. Pain Med 2010;11:1274–1277. doi:10.1111/j.1526-4637.2010.00916.x. [PubMed: 20704676]

[44]. Introduction to Parkinson's and Huntington's Disease. CNS Regen 1999:295–298. doi:10.1016/B978-012705070-6/50011-1.

[45]. Jenkinson M, Bannister P, Brady M, Smith S. Improved optimization for the robust and accurate linear registration and motion correction of brain images. Neuroimage 2002;17:825–41. Available: http://www.ncbi.nlm.nih.gov/pubmed/12377157 Accessed 24 May 2018. [PubMed: 12377157]

[46]. Jenkinson M, Bannister P, Brady M, Smith S. Improved optimization for the robust and accurate linear registration and motion correction of brain images. Neuroimage 2002;17:825–41. Available: http://www.ncbi.nlm.nih.gov/pubmed/12377157 Accessed 14 Nov 2017. [PubMed: 12377157]

[47]. Kazis LE, Miller DR, Skinner KM, Lee A, Ren XS, Clark JA, Rogers WH, Sprio A, Selim A, Linzer M, Payne SMC, Mansell D, Fincke BG. Applications of methodologies of the Veterans Health Study in the VA healthcare system: conclusions and summary. J Ambul Care Manage 2006;29:182–8. Available: http://www.ncbi.nlm.nih.gov/pubmed/16552327 Accessed 26 Aug 2018. [PubMed: 16552327]

[48]. Kim J-H, Choi S-H, Jang JH, Lee D-H, Lee K-J, Lee WJ, Moon JY, Kim YC, Kang D-H. Impaired insula functional connectivity associated with persistent pain perception in patients with complex regional pain syndrome. PLoS One 2017;12:e0180479. doi:10.1371/journal.pone.0180479.

[49]. Kim J, Loggia ML, Edwards RR, Wasan AD, Gollub RL, Napadow V. Sustained deep-tissue pain alters functional brain connectivity. Pain 2013;154:1343–51. doi:10.1016/j.pain.2013.04.016. [PubMed: 23718988]

[50]. Kim W, Kim SK, Nabekura J. Functional and structural plasticity in the primary somatosensory cortex associated with chronic pain. J Neurochem 2017;141:499–506. [PubMed: 28278355]

[51]. Kohler M, Strauss S, Horn U, Langner I, Usichenko T, Neumann N, Lotze M. Differences in Neuronal Representation of Mental Rotation in Patients With Complex Regional Pain Syndrome and Healthy Controls. J Pain 2019;20:898–907. doi:10.1016/j.jpain.2019.01.330. [PubMed: 30710707]

[52]. Lebel A, Becerra L, Wallin D, Moulton EA, Morris S, Pendse G, Jasciewicz J, Stein M, Aiello-Lammens M, Grant E, Berde C, Borsook D. fMRI reveals distinct CNS processing during symptomatic and recovered complex regional pain syndrome in children. Brain 2008;131:1854–1879. doi:10.1093/brain/awn123. [PubMed: 18567621]

[53]. Lenz M, Hoffken O, Stude P, Lissek S, Schwenkreis P, Reinersmann A, Frettloh J, Richter H, Tegenthoff M, Maier C. Bilateral somatosensory cortex disinhibition in complex regional pain syndrome type I. Neurology 2011;77:1096–1101. doi:10.1212/WNL.0b013e31822e1436. [PubMed: 21880999]

[54]. Linnman C, Becerra L, Lebel A, Berde C, Grant PE, Borsook D. Transient and Persistent Pain Induced Connectivity Alterations in Pediatric Complex Regional Pain Syndrome. PLoS One 2013;8:e57205. doi:10.1371/journal.pone.0057205.

[55]. Loher TJ, Burgunder J-M, Weber S, Sommerhalder R, Krauss JK. Effect of chronic pallidal deep brain stimulation on off period dystonia and sensory symptoms in advanced Parkinson's disease. J Neurol Neurosurg Psychiatry 2002;73:395–9. doi:10.1136/jnnp.73.4.395. [PubMed: 12235307]

[56]. Maihofner C, Baron R, DeCol R, Binder A, Birklein F, Deuschl G, Handwerker HO, Schattschneider J. The motor system shows adaptive changes in complex regional pain syndrome. Brain 2007;130:2671–2687. doi:10.1093/brain/awm131. [PubMed: 17575278]

[57]. Maihöfner C, Forster C, Birklein F, Neundörfer B, Handwerker HO. Brain processing during mechanical hyperalgesia in complex regional pain syndrome: a functional MRI study. Pain 2005;114:93–103. doi:10.1016/j.pain.2004.12.001. [PubMed: 15733635]

[58]. Mancini F, Wang AP, Shira MM, Isherwood ZJ, McAuley JH, Iannetti G, Sereno MI, Moseley L, Rae CD. Preserved cortical maps of the body in Complex Regional Pain Syndrome. bioRxiv 2018:409094.

[59]. Manjón J V, Coupé P, Martí-Bonmatí L, Collins DL, Robles M. Adaptive non-local means denoising of MR images with spatially varying noise levels. J Magn Reson Imaging 2010;31:192–203. doi:10.1002/jmri.22003. [PubMed: 20027588]

[60]. Mansour AR, Farmer MA, Baliki MN, Apkarian AV. Chronic pain: The role of learning and brain plasticity. Restor Neurol Neurosci 2014;32:129–139. [PubMed: 23603439]

[61]. Di Martino A, Scheres A, Margulies DS, Kelly AMC, Uddin LQ, Shehzad Z, Biswal B, Walters JR, Castellanos FX, Milham MP. Functional Connectivity of Human Striatum: A Resting State fMRI Study. Cereb Cortex 2008;18:2735–2747. doi:10.1093/cercor/bhn041. [PubMed: 18400794]

[62]. Martucci KT, Ng P, MacKey S. Neuroimaging chronic pain: What have we learned and where are we going? Future Neurol 2014;9:615–626. [PubMed: 28163658]

[63]. Mathiowetz V, Weber K, Kashman N, Volland G. Adult norms for the Nine Hole Peg Test of finger dexterity. Occup Ther J Res 1985;5:24–38. Available: https://experts.umn.edu/en/publications/adult-norms-for-the-nine-hole-peg-test-of-finger-dexterity Accessed 14 Nov 2017.

[64]. Miller LK, Jerosch-Herold C, Shepstone L. Clinical assessment of hand oedema: A systematic review. Hand Ther 2017;22:153–164. doi:10.1177/1758998317724405.

[65]. Moulton EA, Schmahmann JD, Becerra L, Borsook D. The cerebellum and pain: passive integrator or active participator? Brain Res Rev 2010;65:14–27. doi:10.1016/j.brainresrev.2010.05.005. [PubMed: 20553761]

[66]. Munts AG, Mugge W, Meurs TS, Schouten AC, Marinus J, Moseley GL, van der Helm FCT, van Hilten JJ. Fixed dystonia in complex regional pain syndrome: a descriptive and computational modeling approach. BMC Neurol 2011;11:53. doi:10.1186/1471-2377-11-53. [PubMed: 21609429]

[67]. Munts AG, Van Rootselaar A-F, Van Der Meer JN, Koelman JHTM, Van Hilten JJ, Tijssen MAJ. Clinical and neurophysiological characterization of myoclonus in complex regional pain syndrome. Mov Disord 2008;23:581–587. doi:10.1002/mds.21910. [PubMed: 18163455]

[68]. Napadow V, LaCount L, Park K, As-Sanie S, Clauw DJ, Harris RE. Intrinsic brain connectivity in fibromyalgia is associated with chronic pain intensity. Arthritis Rheum 2010;62:2545–2555. doi:10.1002/art.27497. [PubMed: 20506181]

[69]. Neychev VK, Gross RE, Lehéricy S, Hess EJ, Jinnah HA. The functional neuroanatomy of dystonia. Neurobiol Dis 2011;42:185–201. doi:10.1016/j.nbd.2011.01.026. [PubMed: 21303695]

[70]. Owens-Walton C, Jakabek D, Li X, Wilkes FA, Walterfang M, Velakoulis D, van Westen D, Looi JCL, Hansson O. Striatal changes in Parkinson disease: An investigation of morphology, functional connectivity and their relationship to clinical symptoms. Psychiatry Res Neuroimaging 2018;275:5–13. doi:10.1016/j.pscychresns.2018.03.004. [PubMed: 29555381]

[71]. Peyron R, Schneider F, Faillenot I, Convers P, Barral F-G, Garcia-Larrea L, Laurent B. An fMRI study of cortical representation of mechanical allodynia in patients with neuropathic pain. Neurology 2004;63:1838–46. doi:10.1212/01.wnl.0000144177.61125.85. [PubMed: 15557499]

[72]. Di Pietro F, McAuley JH, Parkitny L, Lotze M, Wand BM, Moseley GL, Stanton TR. Primary Motor Cortex Function in Complex Regional Pain Syndrome: A Systematic Review and Meta-Analysis. J Pain 2013;14:1270–1288. doi:10.1016/J.JPAIN.2013.07.004. [PubMed: 24035350]

[73]. Di Pietro F, McAuley JH, Parkitny L, Lotze M, Wand BM, Moseley GL, Stanton TR. Primary Somatosensory Cortex Function in Complex Regional Pain Syndrome: A Systematic Review and Meta-Analysis. J Pain 2013;14:1001–1018. doi:10.1016/j.jpain.2013.04.001. [PubMed: 23726046]

[74]. Pleger B, Tegenthoff M, Schwenkreis P, Janssen F, Ragert P, Dinse HR, Völker B, Zenz M, Maier C. Mean sustained pain levels are linked to hemispherical side-to-side differences of primary somatosensory cortex in the complex regional pain syndrome I. Exp Brain Res 2004;155:115–119. doi:10.1007/s00221-003-1738-4. [PubMed: 15064892]

[75]. Porcu M, Craboledda D, Garofalo P, Barberini L, Sanfilippo R, Zaccagna F, Wintermark M, Montisci R, Saba L. Reorganization of brain networks following carotid endarterectomy: an exploratory study using resting state functional connectivity with a focus on the changes in Default Mode Network connectivity. Eur J Radiol 2019;110:233–241. doi:10.1016/j.ejrad.2018.12.007. [PubMed: 30599866]

[76]. Power JD, Mitra A, Laumann TO, Snyder AZ, Schlaggar BL, Petersen SE. Methods to detect, characterize, and remove motion artifact in resting state fMRI. Neuroimage 2014;84:320–41. doi:10.1016/j.neuroimage.2013.08.048. [PubMed: 23994314]

[77]. Pruim RHR, Mennes M, van Rooij D, Llera A, Buitelaar JK, Beckmann CF. ICA-AROMA: A robust ICA-based strategy for removing motion artifacts from fMRI data. Neuroimage 2015;112:267–277. doi:10.1016/j.neuroimage.2015.02.064. [PubMed: 25770991]

[78]. Rajapakse JC, Giedd JN, Rapoport JL. Statistical approach to segmentation of single-channel cerebral MR images. IEEE Transactions on Medical Imaging.1997, Vol. 16 pp. 176–186. doi:10.1109/42.563663. [PubMed: 9101327]

[79]. van Rijn MA, Marinus J, Putter H, Bosselaar SRJ, Moseley GL, van Hilten JJ. Spreading of complex regional pain syndrome: not a random process. J Neural Transm 2011;118:1301–9. doi:10.1007/s00702-011-0601-1. [PubMed: 21331457]

[80]. Robinson JL, Barron DS, Kirby LAJ, Bottenhorn KL, Hill AC, Murphy JE, Katz JS, Salibi N, Eickhoff SB, Fox PT. Neurofunctional topography of the human hippocampus. Hum Brain Mapp 2015;36:5018–37. doi:10.1002/hbm.22987. [PubMed: 26350954]

[81]. Sesack SR, Grace AA. Cortico-basal ganglia reward network: Microcircuitry. Neuropsychopharmacology 2010;35:27–47. [PubMed: 19675534]

[82]. Shroff S. Caudate Nucleus Encyclopedia of Clinical Neuropsychology. New York, NY: Springer New York, 2011 pp. 504–506. doi:10.1007/978-0-387-79948-3_302.

[83]. Smallwood RF, Laird AR, Ramage AE, Parkinson AL, Lewis J, Clauw DJ, Williams DA, Schmidt-Wilcke T, Farrell MJ, Eickhoff SB, Robin DA. Structural brain anomalies and chronic pain: a quantitative meta-analysis of gray matter volume. J Pain 2013;14:663–75. doi:10.1016/j.jpain.2013.03.001. [PubMed: 23685185]

[84]. Smith SM. Fast robust automated brain extraction. Hum Brain Mapp 2002;17:143–155. doi:10.1002/hbm.10062. [PubMed: 12391568]

[85]. Stoodley CJ, Schmahmann JD. Evidence for topographic organization in the cerebellum of motor control versus cognitive and affective processing. Cortex 2010;46:831–44. doi:10.1016/j.cortex.2009.11.008. [PubMed: 20152963]

[86]. Tanaka S, Kirino E. Functional Connectivity of the Dorsal Striatum in Female Musicians. Front Hum Neurosci 2016;10:178. doi:10.3389/fnhum.2016.00178. [PubMed: 27148025]

[87]. Thibes RB, Novaes NP, Lucato LT, Campanholo KR, Melo LM, Leite CC, Amaro E, Barbosa ER, Bor-Seng-Shu E, Cardoso EF, Sato JR. Altered Functional Connectivity Between Precuneus and Motor Systems in Parkinson's Disease Patients. Brain Connect 2017;7:643–647. doi:10.1089/brain.2017.0534. [PubMed: 29065697]

[88]. Tohka J, Zijdenbos A, Evans A. Fast and robust parameter estimation for statistical partial volume models in brain MRI. Neuroimage 2004;23:84–97. doi:10.1016/J.NEUROIMAGE.2004.05.007. [PubMed: 15325355]

[89]. Tomasi D, Volkow ND. Association between functional connectivity hubs and brain networks. Cereb Cortex 2011;21:2003–13. doi:10.1093/cercor/bhq268. [PubMed: 21282318]

[90]. Upadhyay J, Anderson J, Baumgartner R, Coimbra A, Schwarz AJ, Pendse G, Wallin D, Nutile L, Bishop J, George E, Elman I, Sunkaraneni S, Maier G, Iyengar S, Evelhoch JL, Bleakman D, Hargreaves R, Becerra L, Borsook D. Modulation of CNS pain circuitry by intravenous and sublingual doses of buprenorphine. Neuroimage 2012;59:3762–3773. [PubMed: 22119647]

[91]. Verdugo RJ, Ochoa JL. Abnormal movements in complex regional pain syndrome: assessment of their nature. Muscle Nerve 2000;23:198–205. Available: http://www.ncbi.nlm.nih.gov/pubmed/10639611 Accessed 10 Sep 2018. [PubMed: 10639611]

[92]. Woby SR, Roach NK, Urmston M, Watson PJ. Psychometric properties of the TSK-11: A shortened version of the Tampa Scale for Kinesiophobia. Pain 2005;117:137–144. doi:10.1016/j.pain.2005.05.029. [PubMed: 16055269]

[93]. Yager LM, Garcia AF, Wunsch AM, Ferguson SM. The ins and outs of the striatum: Role in drug addiction. Neuroscience 2015;301:529–541. [PubMed: 26116518]

[94]. Zhang Y, Brady M, Smith S. Segmentation of brain MR images through a hidden Markov random field model and the expectation-maximization algorithm. IEEE Trans Med Imaging 2001;20:45–57. doi:10.1109/42.906424. [PubMed: 11293691]

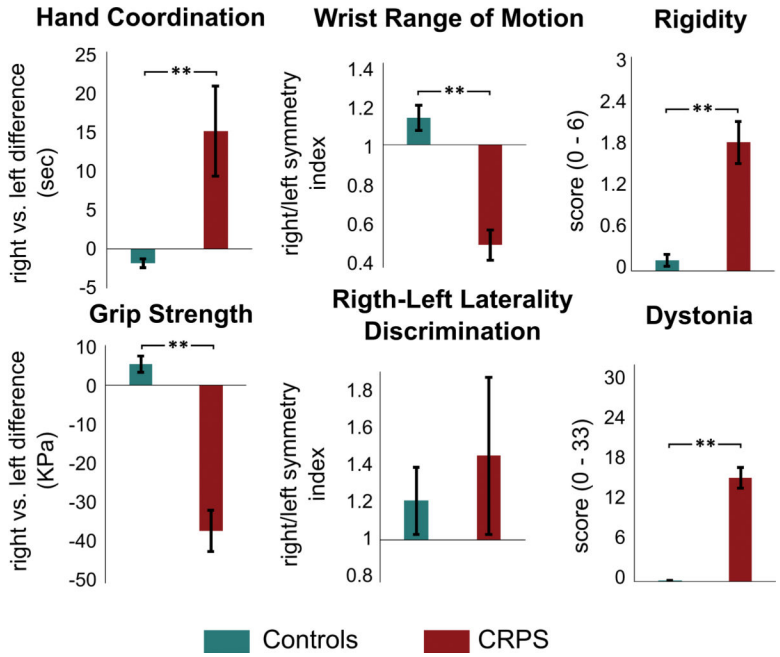

Figure 1. Functional motor tests performance.

CRPS patients presented with significantly (**p < 0.01) substantial motor deficits in the affected hand relative to healthy controls. The functional motor metrics reflect the performance of the affected (dominant, in case of healthy controls) hand in relation to the healthy (non-dominant) hand to account for intragroup variability.

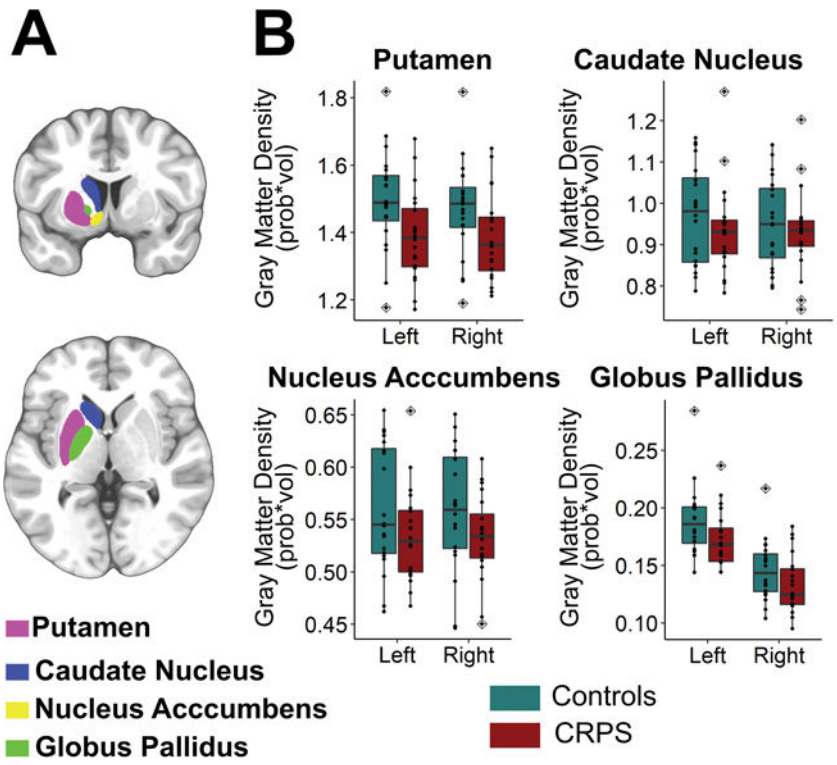

Figure 2. Box plots to show group differences in gray matter density.

Out of all of the striatal ROIs analyzed (A), only the putamen showed a significant bilateral reduction in GMD in chronic CRPS patients when compared to healthy controls. Black dots indicate singe-subjects data. Outlier observations (e.g: outside 1.5 times the interquartile range above the upper quartile and bellow the lower quartile) are denoted with a rhombis symbol. Statistical results stemming from group x side repeated measures ANOVA are given in Table 3.

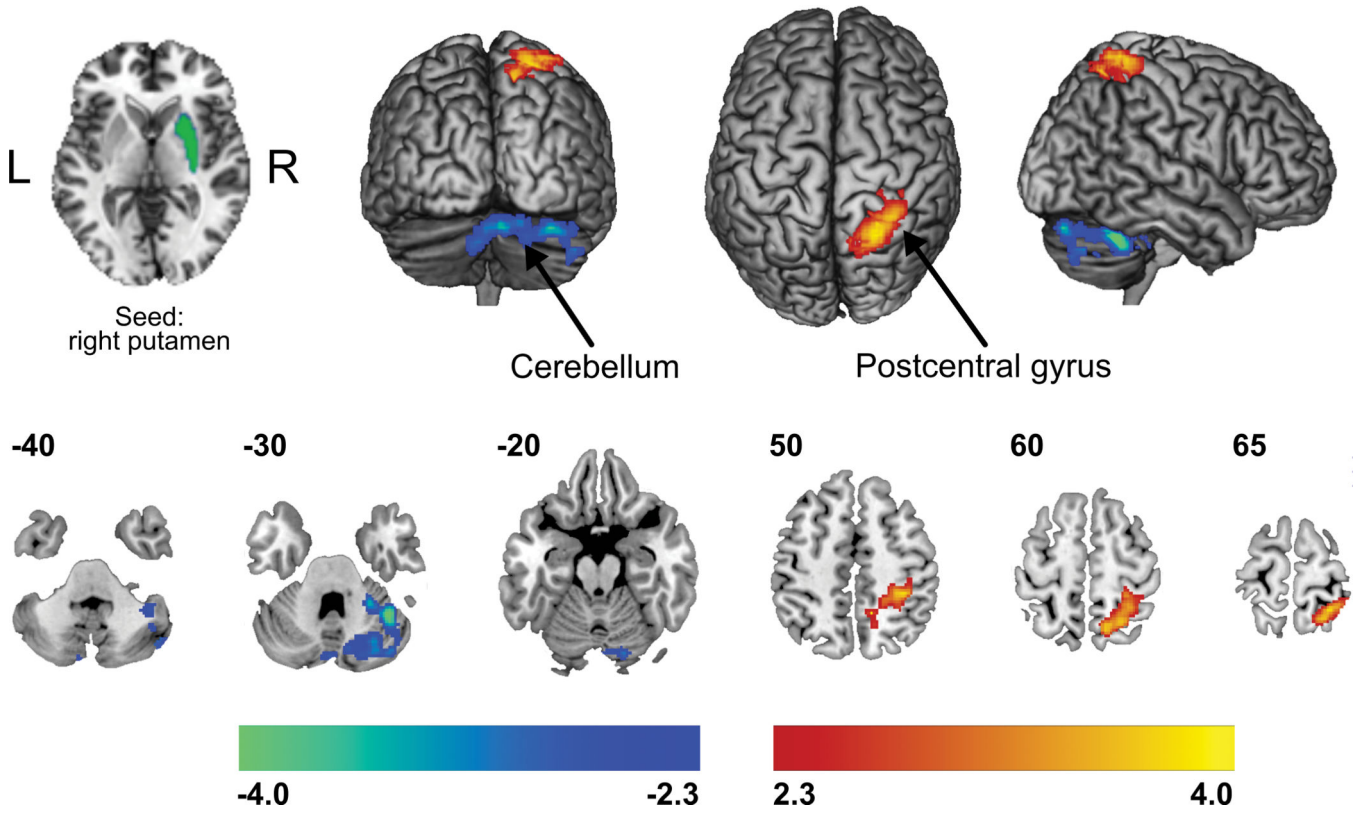

Figure 3. Group differences in resting state functional connectivity of the putamen.

Compared to matched controls, CRPS patients demonstrated greater functional connectivity strength (warm colors) amongst the right (ipsilateral to the affected limb) putamen and sensorimotor and superior parietal cortices, while decreased connectivity (cold colors) was quantified with the crus I region of the cerebellum. Statistical maps were thresholded at p-value < 0.05, corrected for multiple comparisons. Color bars show z-values.

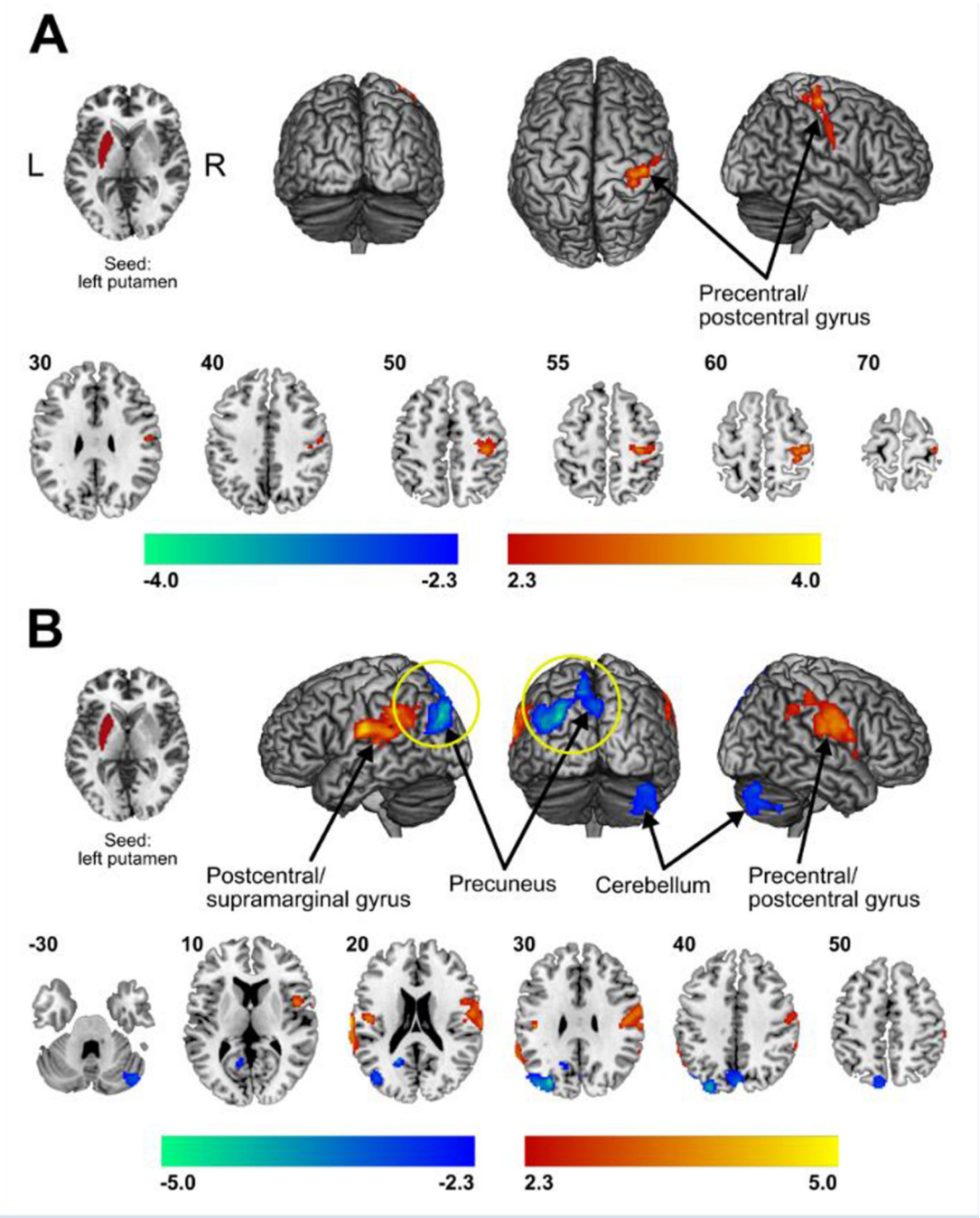

Figure 4. Correlation of resting state functional connectivity of the putamen with behavioral measures.

Patients reporting higher spontaneous pain intensity on the day of the scan showed greater functional connectivity of the left putamen with spread motor and sensory discriminative areas. The pain intensity was reported on a visual scale of 0 = “no pain” to 10 = “worse imaginable pain” (A). Interaction analysis (diseaseXmotor dysfunction) showed that patients with poorer hand and finger coordination, as evaluated with the 9-Hole Peg Test, presented increased functional connectivity strengths (warm colors) amongst the left putamen and motor and discriminative/association areas, as well as decreased functional connectivity

(cold colors) between the left putamen and both the cerebellum (crus I and II) and precuneus (B). Statistical maps were thresholded at p-value < 0.05. Color bars show z-values. Further Correction for multiple comparison using false discovery rate (FDR) showed that only decreases of functional connectivity of putamen with precuneus in the context of poor hand and finger coordination were significant – highlighted with a yellow circle in the figure.

Table 1.

Patient demographics, clinical history and medication information

Patient	Age (y)	Gender	Pain intensity (0–10)	Pain duration (m)	Pain location	Inciting event	Pain medication (doses, frequency)		Over motor deficits
							Analgesic	Co-analgesic	
1	37	female	3	103	right hand	scaphoid fracture, surgery	ibuprofen 600mg, PRN metamizole, PRN	—	weakness limited RoM poor coordination dystonia
2	46	female	2	80	right hand	carpal tunnel syn., surgery	metamizole, 500mg, PRN	—	weakness limited RoM
3	53	female	9	39	right hand	CMC osteoarthritis, surgery	—	—	weakness limited RoM poor coordination dystonia
4	54	female	1	11	right hand	finger cut with blood poisoning	metamizole 500mg, QD tramadol 500mg, QD	gabapentin 300mg, BID	weakness poor coordination dystonia
5	55	female	6	109	right arm	elbow surgery	—	—	weakness limited RoM poor coordination dystonia
6	57	female	4	50	right hand	carpal tunnel syn., surgery	ibuprofen 800mg, QD metamizole, QD tapentadol 100mg, BID	duloxetine 30mg, QD	weakness poor coordination rigidity dystonia
7	57	female	3	8	right hand	radius fracture, cast	—	—	rigidity
8	58	female	5	15	right hand, forearm	epicondylitis with partial tear	—	—	rigidity
9	62	female	8	7	right arm	radius fracture	metamizole, BID	tramadol, BID	weakness limited RoM rigidity dystonia
10	64	female	1	19	right hand	radius fracture, surgery	—	—	rigidity
11	66	female	4	6	right hand	radius fracture	metamizole 500mg, TID tilidine 50/4, BID	amitriptyline, QD	weakness limited RoM dystonia
12	67	female	5	140	right hand, forearm	radius fracture, cast	—	—	weakness limited RoM poor coordination
13	67	female	2	105	right hand	dislocated shoulder, surgery	ibuprofen 800mg, PRN	pregabalin 150mg, BID	—

Pain. Author manuscript; available in PMC 2021 March 01.

Patient	Age (y)	Gender	Pain intensity (0–10)	Pain duration (m)	Pain location	Inciting event	Pain medication (doses, frequency)		Over motor deficits
							Analgesic	Co-analgesic	
14	69	female	6	144	right hand	radius fracture, surgery	ibuprofen 600mg, PRN aspirin 100mg, PRN	—	weakness
15	71	female	4	126	right hand	radius fracture	aspirin 500mg, PRN metamizole 500mg, PRN tramadol 100mg, PRN	—	limited RoM
16	47	male	8	57	right arm	radius head fracture	oxycodone 5mg, PRN	—	weakness limited RoM poor coordination rigidity dystonia
17	51	male	7	13	right hand, forearm	radius fracture, surgery	metamizole 500mg, PRN tilidine 50/4, BID	gabapentin 200mg, BID duloxetine, PRN	weakness limited RoM poor coordination dystonia
18	53	male	6	18	right arm	ulna fracture, surgery	ibuprofen 600mg, BID metamizolde 500mg, QD	—	weakness limited RoM poor coordination dystonia
19	56	male	4	64	right arm	TMC osteoarthritis, surgery	metamizole, BID	pregabalin 75mg, BID	weakness poor coordination dystonia
20	67	male	4	77	right hand	radius fracture, surgery	—	—	weakness

CMC: Carpometacarpal; TMC: trapeziometacarpal; QD: once a day; BID: twice a day; PRN: as needed; RoM: forearm range of motion

Table 2.

Group comparison of somatosensory evaluation, autonomic function and psychometrics.

	CRPS Patients		Healthy Controls		p-value
Number of patients, N	20		20		-
Somatosensory evaluation					
Monofilament test right, N (%)	7	(35%)	1	(5%)	**0.010** [a]
Monofilament test left, N (%)	4	(20%)	1	(5%)	0.171 [a]
2-point discrimination test right, N (%)	3	(15%)	1	(5%)	0.302 [a]
2-point discrimination test left, N (%)	0	(0%)	0	(0%)	
Autonomic function					
Abnormal sweating pattern, N (%)	19	(95%)	0	(0%)	**< 0.001** [a]
Abnormal nail growth pattern, N (%)	12	(60%)	0	(0%)	**< 0.001** [a]
Abnormal hair growth pattern, N (%)	4	(20%)	0	(0%)	0.053 [a]
Abnormal skin color, N (%)	14	(70%)	0	(0%)	**< 0.001** [a]
Abnormal hand volume, N (%)	12	(60%)	4	(25%)	**0.038** [a]
Abnormal hand temperature, N (%)	8	(40%)	3	(15%)	0.078 [a]
Quality of life					
Veterans RAND 12 PCS, Mean (SE)	34.52	(1.80)	53.47	(0.98)	**< 0.001** [b]
Veterans RAND 12 MCS, Mean (SE)	45.80	(3.39)	55.35	(1.76)	**0.025** [b]
Mental health					
HADS depression, Median (IQR) | N(%)	6 (6)	| 9 (45%)	2 (4)	| 0 (0%)	**0.001** [a]
HADS anxiety, Median (IQR) | N(%)	5 (5)	| 7 (35%)	4 (3)	| 2 (10%)	0.058 [a]
Kinesiophobia					
TSK-11, Median (IQR) | N (%)	22 (11)	| 6 (30%)	13(4)	| 1 (5%)	**< 0.001** [a]

N: Number of participants presenting with abnormal scores

% : Percentage of participants presenting with abnormal scores

SE: Standard Error; IQR: Inter quartile range

PCS: Physical Composite Score; MCS: Mental Composite Score

HADS : Hospital Anxiety and Depression Scale, range: 0–21

TSK-11 Tampa Scale Kinesiophobia, range: 11–44

[a] One tail Fisher Test

[b] Mann Whitney Test

Table 3.

Group (CRPS and healthy controls) x side (left and right hemisphere) comparison of striatal volumes with mixed-design analysis of variance (ANOVA).

Effect	*df*	*SS*	*MS*	*F-value*	*p-value*
Putamen					
Group	1	0.176	0.176	4.717	**0.036**
Error (Group)	38	1.417	0.037		
Side	1	0.00415	0.004153	3.842	0.057
Side x Group	1	0.00275	0.00275	2.544	0.119
Error (Side x Group)	38	0.04107	0.001081		
Caudate Nucleus					
Group	1	0.0147	0.01465	0.615	0.438
Error (Group)	38	0.9055	0.02383		
Side	1	0.004476	0.004476	6.332	**0.0162**
Side x Group	1	0.001145	0.001145	1.619	0.211
Error (Side x Group)	38	0.02686	0.000707		
Nucleus Accumbens					
Group	1	0.01353	0.013528	2.669	0.111
Error (Group)	38	0.19262	0.005069		
Side	1	0.000094	9.40E-05	0.314	0.579
Side x Group	1	0.000015	1.45E-05	0.049	0.827
Error (Side x Group)	38	0.011378	2.99E-04		
Globus Pallidus					
Group	1	0.00364	0.003638	2.758	0.105
Error (Group)	38	0.05013	0.001319		
Side	1	0.03359	3.36E-02	369.969	**<2e-16**
Side x Group	1	0.00003	3.00E-05	0.335	0.566
Error (Side x Group)	38	0.00345	9.00E-05		

df: degrees of freedom; SS: Sum of Squares; MS: Mean Square

Table 4.

Regions in which seed-based resting functional connectivity strengths were significantly different between CRPS patients and healthy controls. Note that "seed" clusters were derived from the previous gray matter volume analyses. Locations are in Montreal Neurological Institute space. Significant clusters were formed with cluster-extent thresholding (family-wise error rate) to correct for multiple comparisons.

	X	Y	Z	z-statistic	cluster	cluster size	p-value
crps > controls							
seed: right putamen							
right primary somatosensory cortex	20	−54	64	3.94	1	1545	0.00061
right superior parietal lobe	12	−50	50	3.86			
crps < controls							
seed: right putamen							
right cerebellum crus1	4.48	40	−52	−32	1	1448	0.00099
pain intensity (positive) correlation							
seed: left putamen							
right primary somatosensory	34	−32	60	3.15	1	735	0.02720
right primary motor cortex	32	−24	54	3.49			
dystonia (positive) correlation							
seed: left putamen							
left supramarginal gyrus	−52	−46	24	3.40	1	892	0.01010
Hand coordination, crps > controls							
seed: left putamen							
left postcentral gyrus	−67	−15	20	4.45	1	992	0.00339
left supramarginal gyrus	−64	−40	17	3.83			
right premotor cortex	48	2	14	4.11			
right precentral gyrus	58	−8	34	3.64	2	1482	0.00069
right postcentral gyrus	66	−18	20	3.60			
Hand coordination, crps < controls							
seed: left putamen							
left precuneus	−10	−84	52	4.27	1	1893	0.00000
left lateral occipital cortex	−30	−80	32	5.39			
right cerebellum crus I	42	−74	−28	3.39	2	784	0.03320
right cerebellum crus II	48	−70	−42	3.24			
Forearm range of motion, crps < controls							
seed: right putamen							

	X	Y	Z	z-statistic	cluster	cluster size	p-value
left precentral gyrus	−60	−4	14	3.80	1	907	0.01620
left postcentral gyrus	−50	−16	18	4.34			